Journal of Crystal Growth 386 (2014) 179–182

Contents lists available at ScienceDirect

Journal of Crystal Growth

journal homepage: www.elsevier.com/locate/jcrysgro

Spatially-controlled protein crystallization in microfluidic chambers

Clothilde Longuet [a,b,c], Ayako Yamada [a,b,c], Yong Chen [a,b,c], Damien Baigl [a,b,c], Jacques Fattaccioli [a,b,c,*]

[a] Département de Chimie, Ecole Normale Supérieure, 24 rue Lhomond, 75005 Paris, France
[b] CNRS U.M.R. 8640 P.A.S.T.E.U.R., 24 rue Lhomond, 75005 Paris, France
[c] Université Pierre et Marie Curie (UPMC), 4 place Jussieu, 75005 Paris, France

ARTICLE INFO

Article history:
Received 3 September 2013
Received in revised form
7 October 2013
Accepted 8 October 2013
Communicated by S.R. Qiu
Available online 16 October 2013

Keywords:
A1. Crystallization
A1. Nucleation
Microfluidics
Spatial control
Oil/water interface
HEW lysozyme

ABSTRACT

We present a simple microfluidic device able to trigger the nucleation of the crystals at specific locations on the microchip for the statistical study of protein crystallization. The microsystem is an array of independent PDMS microchambers connected to a fluid-dispensing channel. The chambers are filled with a crystallizing aqueous protein solution and then sealed with a fluorinated oil phase. Each chamber presents a small oil/water interface at the connection with the main channel. The crystals most likely grow near the interface, allowing a microscopic observation of the nucleation events at specific positions on the chip. For the sake of demonstration, the method is applied to the crystallization of HEW lysozyme.

1. Introduction

Protein crystals are three-dimensional arrays of macromolecules in which every molecule or specific group of molecules has the same orientation and relationship to its neighbors. Starting from the first crystallization experiment of hemoglobin achieved by Hünefeld in 1840, the rationale of the fabrication of protein crystals has slowly shifted from purification needs towards the theoretical studies of crystallization and the structural determination of proteins and protein complexes [1].

The multidimensional phase diagram of a protein depends on a wide range of physico-chemical parameters such as the solution composition, the nature of the precipitating agent, the pH and the ionic strength, the temperature, etc. To crystallize, a protein solution should be in a supersaturated, metastable state of its phase diagram, in a region where nucleation and growth are permitted and amorphous precipitation forbidden [2].

Obtaining an acceptable protein crystal is an empirical, trial- and error based procedure, and several crystallization techniques have been developed so far (vapor-diffusion, free-interface diffusion, dialysis, etc.) [1,2] to allow the protein solution to follow different kinetic crystallization paths within the phase diagram.

Systems where the crystallizing solution is directly in contact with the surface of the vessel are likely to promote defect-induced heterogeneous nucleation [3–5] which can be detrimental for the quality of the crystals. To avoid this, the microbatch technique, a container-free, high-throughput crystal growth screening method [6] has been developed. In brief, a small aqueous droplet of supersaturated protein crystallizing solution, containing a precipitant, is encapsulated in an organic oil used as a sealant to avoid evaporation. The crystallization occurs in a molecularly smooth liquid vessel, and it has been shown recently that the nature of the oil greatly influences the apparition of crystals [7].

Microfluidics and more generally lab-on-a-chip technologies offer a wide range of possibilities in the domain of protein crystallization. The ability to manipulate fluids at the pico- to the nanoliter scale, using valves [8], droplets [9,10] or wells [11–13], makes possible the replication of the classical techniques with a high-throughput screening of the crystallization conditions, a lower product consumption and a greater control of the transport phenomena [14]. Microchips can be used for formulation purposes, i.e. construction of phase diagrams and crystal growth [8,9,11–13,15], or for fundamental studies of protein crystallization [16].

The apparition of a protein crystal is a statistical event and the measurement of the time distribution of the nucleation process necessitates the parallel study of several identical vessels of

* Corresponding author at: Département de Chimie, Ecole Normale Supérieure, 24 rue Lhomond, 75005 Paris, France. Tel.: +33 1 44 32 24 28.
E-mail address: jacques.fattaccioli@ens.fr (J. Fattaccioli).

0022-0248/$ - see front matter © 2013 Elsevier B.V. All rights reserved.
http://dx.doi.org/10.1016/j.jcrysgro.2013.10.011

crystallizing solution. Well-based devices are usually simpler to design, to use and to analyze [17] but the defects of the walls increase the occurrence of heterogeneous crystallization. Droplet-based microdevices, however, show no surface-defects but are more difficult to fabricate since flow controls and specific surfactants [18] are necessary to create and stabilize the droplets.

In this article, we present a hybrid microfluidic device that takes the advantages of both of the above designs [19,20]: the microsystem is an array of 70 circular PDMS microchambers loaded with the crystallization solution and sealed by a surfactant-free fluorinated oil phase that sits within the main channel. Each chamber is closed by a small oil/precipitating solution interface that triggers nucleation in its vicinity and allows the spatial control of the crystal position on the chip with a sub-10 μm resolution.

2. Materials and methods

2.1. Protein crystallization solution

The protein solution contains 35 mg mL^{-1} of HEW lysozyme (EC Number 235-747-3) diluted in an acetate buffer (pH=4.5, 10 mmol L^{-1}). Sodium chloride (NaCl) was chosen as the precipitating agent at a concentration of 1 mol L^{-1}. The sealing oil is a fluorinated Fluorinert FC-40 oil ($C_{21}F_{48}N_2$). All chemicals were purchased from Sigma-Aldrich and were used as received, without further treatment nor purification. Ultrapure water (Millipore, 18.2 MΩ cm^{-1}) was used for all experiments.

2.2. Fabrication of the microfluidic chip

The protocol used for fabrication was adapted from Yamada et al. [19]. The two-layers device, sketched in Fig. 1, is fabricated in poly(dimethylsiloxane) (PDMS) using soft-lithographic techniques [19,21]. For the bottom layer that contains the channel and the microchambers, PDMS (RTV 615, 10:1 ratio, GE Silicones Co.) was molded on a master fabricated on a silicon wafer using a negative photoresist (SU-8 3050; MicroChem). Microchannels of 50 μm height were patterned on the photoresist by photolithography and hard-baking, following the process from the manufacturer. Then, liquid PDMS was poured onto the mold, degassed and cured at 75 °C for more than 2 h to allow the reticulation to take place. The bottom layer incorporates an array of 70 circular microchambers connected to the main channel by a small neck as shown in Fig. 1. For these experiments, the diameter of the chambers is set to 100 μm and the neck has a rectangular cross section of $15 \times 20\ \mu m^2$. To fabricate the upper part of the chip, that will ultimately serve as an osmotic reservoir, a ca. 5 mm thick PDMS layer was degassed and cured in a plastic petri dish prior to punching a 6 mm diameter hole into it. The two layers of the chip are cut and glued together with uncured PDMS so that the hole of the upper layer covers all of the micro-chambers in the lower layer. This two-layer PDMS block is then baked on a hot plate at 95 °C for 5 min to cure the PDMS glue. The inlet and outlet holes are punched and the PDMS device is bonded to a glass coverslip using an oxygen plasma. Finally, the assembled device is baked on a hot plate at 150 °C for 1 h to make the PDMS wall of the channel recover their hydrophobicity lost during the plasma process [19].

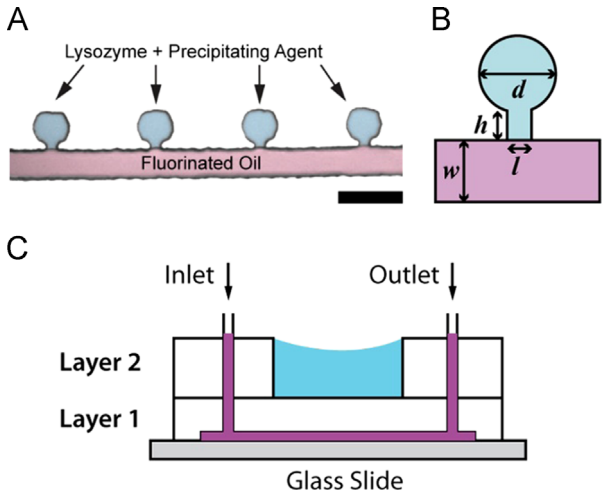

Fig. 1. (A) The chip is made from 70 microchambers, each containing a 35 mg mL^{-1} supersaturated solution of HEW lysozyme in an acetate buffer (pH=4.5) with 1 mol L^{-1} NaCl (blue), separated by a main channel filled with a FC-40 fluorinated oil (pink). Scalebar: 100 μm. (B) In our experiments, the chambers have a diameter $d=100$ μm, a neck length $h=15$ μm and a neck width $l=20$ μm. The main channel has a width equal to $w=80$ μm and the height of all the structures is equal to 50 μm. (C) The microdevice is made from two layers: the lower layer contains the microchambers and the upper layer is used as an osmotic reservoir filled with an acetate buffer solution with 1 mol L^{-1} NaCl. The channel and the reservoir are separated by a piece of PDMS through which the water can diffuse [22]to equilibrate their respective osmotic pressures. (For interpretation of the references to color in this figure legend, the reader is referred to the web version of this article.)

2.3. Microscopy and image analysis

We used a Zeiss Axio observer inverted microscope equipped with an EM-CCD camera, PhotonMAX (Princeton Instruments). All image analyses were done with the ImageJ software.

3. Results and discussion

The microfluidic chip is composed of two PDMS layers having different functions and structures, as sketched in Fig. 1C: the bottom layer incorporates an array of 70 circular crystallization microchambers connected to a main channel by a small neck, as shown in Fig. 1A. For these experiments, as shown in Fig. 1B, the diameter of the chambers is set to 100 μm, the neck has a rectangular cross section of $15 \times 20\ \mu m^2$, and the height of the structures is set to 50 μm.

The upper layer plays the role of an osmotic reservoir that will be detailed further. The crystallization solution, depicted in blue in Fig. 1A, is introduced in the microdevice with the help of a syringe pump (Harvard Apparatus) at a 30 μL min^{-1} flow rate until all the chambers are filled with it, as shown in Fig. 2. Since PDMS is permeable to gas [22] and the outlet is closed, the air in the chambers is gradually pushed out thanks to the pressure of the solution, and totally replaced by the crystallization solution in a short time.

The sealing of the microchambers is done by injecting a fluorinated oil with the microsyringe pump at a flow rate of 25 μL min^{-1}. This flow rate has been optimized to avoid the pressure-driven deformation of the channels and to allow the oil/water interface to be positioned at the neck of the chambers, as shown in Fig. 1A. At the end of the injection, the inlet and outlet tubes are disconnected from the microchip so that the pressure equilibrium is able to avoid any oil movement in the microchannel. According to the manufacturer (3M Company), water in oil and oil in water share the same very low solubility of about 5 mg kg^{-1} which is lower than any of the oil used in previous microbatch studies [7]. The device is thus an array of identical and independent microchambers.

Lysozyme is a 14.7 kDa, 129 aminoacid residues enzyme, present in the mucosal secretion such as saliva and tears and also in chicken egg-white. The catalytic activity is non-specifically

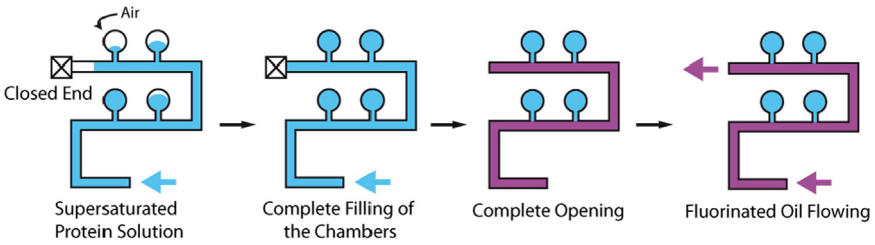

Fig. 2. The crystallization solution is introduced with a syringe pump at a 30 μL min^{-1} flow rate so that the air is totally replaced by the liquid. Then, the fluorinated oil is pushed at a flow rate of 25 μL min^{-1} within the channel to seal the microchambers.

targeted to the gram-positive bacterial cell membranes [23]. For the sake of demonstration, we chose HEW lysozyme as the model protein due to its facility to crystallize and its very well referenced physico-chemical properties in the literature. The supersaturated protein solution contains 35 mg mL^{-1} of HEW lysozyme diluted in an acetate buffer (pH=4.5, 10 mmol L^{-1}). Sodium chloride (NaCl) was chosen as the precipitating agent [24] at a concentration of 1 mol L^{-1} since it allows the crystallization to occur in a reasonable amount of time for our experiments. Besides the fact that organic solvents are able to diffuse easily within the PDMS, it has also been shown that water is able to pervaporate in the PDMS matrix, leading to the existence of permeation-induced flows [22]. To avoid these phenomena that could lead to a change in the supersaturation conditions, we fill the 6 mm-wide hole of the upper layer of the microchip with a 1 mol L^{-1} sodium chloride solution in acetate buffer half an hour before filling the chambers with the precipitation solution and the oil.

In terms of colligative properties of the solution, the molar concentration of salts is much higher than the lysozyme concentration so the osmotic contribution of the protein to the solution is negligible [25]. The crystallization study takes place on a thermostatic plate of an inverted microscope, at a temperature of 18 °C so that the crystals appear within around 30 min after the sealing of the chambers.

The apparition of the crystals is observed with a low magnitude objective to allow the simultaneous observation of several chambers together, as shown in Fig. 3A. Among the 70 chambers of the microchip, around 60% of them experienced a crystal nucleation and growth as shown by the histogram of Fig. 3C. In the chambers where no crystals are observable, either the interface is not stable and the oil invades the chamber, or no crystallization is observable.

At the end of the experiment, the histogram of Fig. 3D shows that more than 80% of the crystals are located at the neck of the chambers where the oil/water interface remains. Fig. 3B shows pictures of the chambers taken with a high-magnification objective. The crystal lies at the interface between the oil and the precipitation solution and gets trapped in the chambers neck. Our device is thus able to selectively trigger the formation of the crystals at the location of the oil/water interface.

In Fig. 4A, we show the time-lapse recording of the nucleation and growth of a lysozyme crystal within the neck of the microchamber. At the resolution allowed by our microscope setup, we measured the time for apparition of a crystal over all the crystallizing chambers of the microchip. This is possible since all these chambers contain a single crystal so their supersaturation conditions are similar before and after the apparition of the crystals. The nucleation time, defined in our work as the time necessary to have a crystal visible with the microscope, is well described by a gaussian distribution, as shown in Fig. 4B, with an average nucleation time of $t=275\pm150$ s for a 35 mg mL^{-1} HEW lysozyme solution in 1 mol L^{-1} NaCl acetate buffer at 18 °C. The statistics suggests that the underlying crystallization mechanism is of the same nature for all the crystals located at the oil/water interfaces.

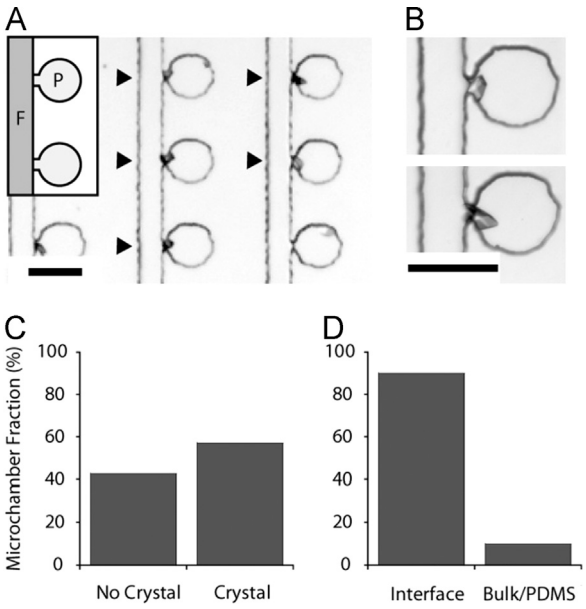

Fig. 3. (A) Protein crystals (indicated by ►) grow mainly in the necks connecting the microchambers filled with the crystallization solution (**P**) to the main channel containing the fluorinated oil (**F**). (B) High-magnification view of the protein crystals after 1 h of incubation. (C) Fraction of microchambers that experienced a crystal growth at the end of the expreriment. (D) Percentage of chambers experiencing crystal growth at the oil/water interface or in the bulk phase and on the PDMS walls. The reported results correspond to data acquired on a single chip. Scale bars=100 μm.

Considering these results, two hypothesis can be made that could explain the high occurrence of the presence of the crystals in the neck of the microchambers. In the first scenario, a nucleus forms in the bulk of the microchamber, by homogeneous or heterogeneous nucleation, and then migrates by diffusion toward the oil/water interface and gets stuck there. In the second one, the nucleation and growth occur both spontaneously near, or at, the interface to lead to larger crystals. The first argument that can be brought in favor of the latter hypothesis is based on colloidal diffusion considerations. The diffusion coefficient of a 100 nm crystal nucleus [5] can be estimated from the Stokes–Einstein coefficient to be close to 5×10^{-8} cm^2 s^{-1} for a viscosity equal to those of water [25,26]. If the nucleation occurs in the bulk phase, the nucleus needs roughly 10^3 s to migrate from the center of the microchamber to its neck. This time is much longer than the average nucleation time measured in Fig. 4B and is not able to explain the time distribution measured. The second argument is related to the presence of the oil/water interface and its effect on the nucleation. Silver et al. published recently an extensive study of the influence of the nature of the oil on crystallization in the case of the microbatch technique [7]. They reported that crystals nucleate and grow near the oil/water interface and that halogenated oils are more likely than other oils to be active towards crystallization and to promote the formation of crystals, although

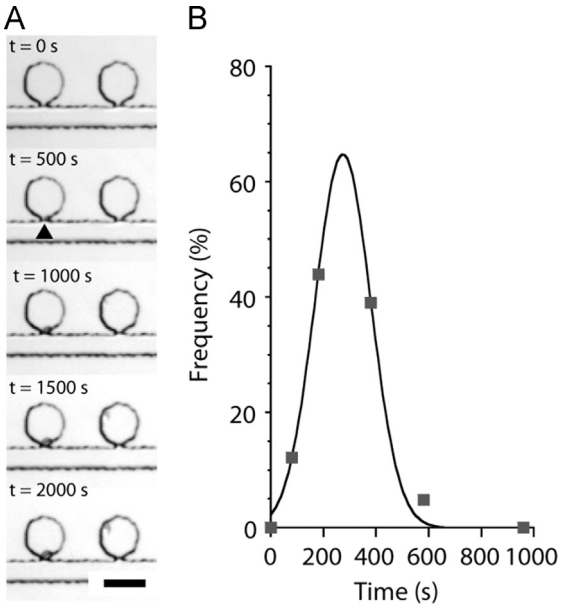

Fig. 4. (A) Time-lapse imaging of the crystal growth (indicated by ►) at the neck of the chambers. This crystal appears at 500 s at the interface. Scale bar = 100 μm. (B) Nucleation frequency with respect to the observation time. The time distribution is well described by a gaussian curve with a mean nucleation time of $t = 275 \pm 150$ s. The reported results correspond to data acquired on a single chip.

the molecular details are not precisely known. We thus conclude that the hypothesis of a nucleation and growth near the interface is the most favorable. In a near future, we plan to use fluorescent techniques [27,28] to perform an in-depth study of the very first moments of nucleation and confirm this scenario. An useful improvement of the microchip would be to develop a design that allows the collection of the crystals directly from the microchambers. This would let the chip to be reused for different experimental conditions and increase its screening capability. Furthermore, the collected crystals could be used as seed to grow bigger ones in a larger chamber and perform on-chip XRD analysis technique [17].

4. Conclusion

We introduced a simple microfluidic device for the study of protein crystallization, made from circular PDMS microchambers. The chambers are first filled with the crystallizing protein solution and then sealed with an oil phase. The existence of oil/water interfaces at the neck of the microchambers causes the protein to nucleate and grow a single crystal per chamber in its vicinity. In the continuity of previous reports [7,29] and our results, the microchip can serve as an experimental basis for the quantitative study of the influence of the nature of the oil on the kinetics of nucleation and growth. Despite the relative small size of the crystals growing in our chambers, compared to what is necessary for structure determination, our device is able to control with accuracy the location of the crystals on the microchip.

References

[1] A. Ducruix, R. Giegé (Eds.), Crystallization of Nucleic Acids and Proteins, 2d ed., Oxford University Press, Oxford, 1999.
[2] N. Chayen, E. Saridakis, Nat. Methods 5 (2008) 147–153.
[3] T. Kawasaki, H. Tanaka, Proc. Natl. Acad. Sci. USA 2010 (2010) 4–6.
[4] K. Harano, T. Homma, Y. Niimi, M. Koshino, K. Suenaga, L. Leibler, E. Nakamura, Nat. Mater. 11 (2012) 877–881.
[5] P.G. Vekilov, Cryst. Growth Des. 10 (2010) 5007–5019.
[6] N. Chayen, P. Shawstewart, D. Blow, J. Cryst. Growth 122 (1992) 176–180.
[7] B.R. Silver, V. Fülöp, P.R. Unwin, New J. Chem. 35 (2011) 602.
[8] C.L. Hansen, E. Skordalakes, J.M. Berger, S.R. Quake, Proc. Natl. Acad. Sci. USA 99 (2002) 16531.
[9] B. Zheng, L.S. Roach, R.F. Ismagilov, J. Am. Chem. Soc. 125 (2003) 11170–11171.
[10] P. Laval, J.B. Salmon, M. Joanicot, J. Cryst. Growth 303 (2007) 622–628.
[11] W. Du, L. Li, K.P. Nichols, R.F. Ismagilov, Lab. Chip 9 (2009) 2286–2292.
[12] X. Zhou, L. Lau, W.W.L. Lam, S.W.N. Au, B. Zheng, Anal. Chem. 79 (2007) 4924–4930.
[13] G. Juárez-Martínez, P. Steinmann, A.W. Roszak, N.W. Isaacs, J.M. Cooper, Anal. Chem. 74 (2002) 3505–3510.
[14] L. Li, R.F. Ismagilov, Annu. Rev. Biophys. 39 (2010) 139–158.
[15] M.O.A Sommer, S. Larsen, J. Synchrotron Radiat. 12 (2005) 779–785.
[16] P. Laval, A. Crombez, J.-B. Salmon, Langmuir 25 (2009) 1836–1841.
[17] C.L. Hansen, S. Classen, J.M. Berger, S.R. Quake, J. Am. Chem. Soc. 128 (2006) 3142–3143.
[18] L.S. Roach, H. Song, R.F. Ismagilov, Anal. Chem. 77 (2005) 785–796.
[19] A. Yamada, F. Barbaud, L. Cinque, L. Wang, Q. Zeng, Y. Chen, D. Baigl, Small 6 (2010) 2169–2175.
[20] A. Gansen, A.M. Herrick, I.K. Dimov, L.P. Lee, D.T. Chiu, Lab. Chip 12 (2012) 2247–2254.
[21] J.C. McDonald, G.M. Whitesides, Acc. Chem. Res. 35 (2002) 491–499.
[22] E. Verneuil, A. Buguin, P. Silberzan, Europhys. Lett. 68 (2004) 412–418.
[23] G. Alderton, W. Ward, H. Fevold, J. Biol. Chem. 157 (1945) 43.
[24] E.L. Forsythe, R.A. Judge, M.L. Pusey, J. Chem. Eng. Data 44 (1999) 637–640.
[25] P. Atkins, J. de Paula, Physical Chemistry, Oxford Higher Education, Oxford, UK, 2009.
[26] R. Giordano, A. Salleo, S. Salleo, F. Wanderlingh, Phys. Lett. A (1979) 64–66.
[27] T. Matsui, G. Sazaki, H. Hondoh, Y. Matsuura, T. Nakada, K. Nakajima, J. Cryst. Growth 293 (2006) 415–422.
[28] J. Sumida, J. Cryst. Growth 232 (2001) 308–316.
[29] N.E. Chayen, Structure 5 (1997) 1269–1274.